Effect of Yttrium Addition on Mechanical Properties for V-4Cr-4Ti Alloy Contaminated with Oxygen and Nitrogen Impurities

Takeshi MIYAZAWA, Takuya NAGASAKA[1)], Yoshimitsu HISHINUMA[1)], Takeo MUROGA[1)], Yanfen LI[2)], Yuhki SATOH[2)], Sawoong KIM[3)] and Hiroaki ABE[2)]

The Graduate University for Advanced Studies, Toki, Gifu 509-5292, Japan
[1)]*National Institute for Fusion Science, Toki, Gifu 509-5292, Japan*
[2)]*Institute for Materials Research, Tohoku University, Sendai 980-8577, Japan*
[3)]*National Fusion Research Institute, Daejeon 305-806, Korea*

(Received 27 June 2013 / Accepted 19 October 2013)

Reduction of interstitial impurities such as nitrogen (N) and oxygen (O) improves the mechanical properties of V-4Cr-4Ti alloys. Yttrium (Y) addition effectively reduces O content by Y_2O_3 slag-out on the melting ingot surface. The effects of Y addition on mechanical properties were investigated for V-4Cr-4Ti with N ranging from 0.009 to 0.29 mass% and O ranging from 0.009 to 0.36 mass%. The increase in yield stress (YS) and ultimate tensile stress (UTS) for vanadium alloys was saturated above 0.1 mass% in O content, because Ti precipitates increased with increasing O content regardless of Y addition. Y addition had little effect on YS and UTS of V-4Cr-4Ti alloys at room temperature (RT). However, Y addition improved impact properties of alloys highly doped with O. Y addition did not suppress hardening due to O doping but did increase deformation for crack initiation.

Keywords: low-activation material, blanket structural material, solid solution hardening

DOI: 10.1585/pfr.8.1405166

1. Introduction

V-4Cr-4Ti alloy, which is a vanadium-based alloy containing Chromium (Cr) of 4 mass% and Titanium (Ti) of 4 mass%, is a candidate for blanket structural materials for fusion reactor systems because of its low-activation properties, good resistance to neutron radiation damage, and good high-temperature strength [1]. Nitrogen (N) and oxygen (O) have very high solubility limits of 1.7 mass% and 2.7 mass% at 1000°C in vanadium, and are potent solid solution strengtheners [2, 3]. Carbon (C) has a relatively low solubility limit of 0.047 mass% at 1000°C in vanadium [3]. Most lots of vanadium contain C in excess of the limit and hence V_2C precipitates. Interstitial C remains low in vanadium. The mechanical behavior of V-4Cr-4Ti alloys is, therefore, strongly influenced by solid solution hardening due to interstitial N and O impurities, which are possible contaminants during fabrication and under operation conditions. The effect of N and O on ductile-to-brittle transition temperature (DBTT) for pure vanadium has been reported [4]. The content of N or O over 0.1 mass% raised DBTT above room temperature (RT). Previous tensile tests at RT on vanadium demonstrated that for embrittlement (fracture without plastic deformation) the threshold content of N was 0.24 mass% and that of O was 0.48 mass% [5]. It is widely recognized that control of these impurities is essential for workability and weldability [6]. It has also been clarified that yttrium (Y) addition effectively reduces O content by Y_2O_3 slag-out on the melting ingot surface [7]. The present study seeks to clarify the effect of Y addition on the mechanical properties of V-4Cr-4Ti alloys with high O and N contents.

2. Experiment

Table 1 lists the V-4Cr-4Ti alloys used in this study and their chemical composition. V-4Cr-4Ti-0.019O is the reference V-4Cr-4Ti alloy, called NIFS-HEAT-2, which was fabricated by electron beam melting and vacuum arc re-melting in 166 kg scale [8, 9]. NIFS-HEAT-2 is high-purity large scale ingots developed by National Institute for Fusion Science, Japan. Three 15 kg-scale ingots were fabricated by levitation melting [3]. 30 g-scale buttons and a 200 g-scale ingot were fabricated by arc-melting. N and O contents were controlled by adding high-purity TiN powder which was larger than 10 μm and V_2O_5 powder which was larger than 20 μm. Figure 1 indicates that N content of these materials was systematically changed from 0.009 to 0.29 mass% and that O content was systematically changed from 0.009 to 0.36 mass%.

Y_2O_3 inclusions with 0.5 μm or larger were already observed in the as-melted ingot. They did not decompose during annealing [7]. Two types Ti precipitates were observed in V-4Cr-4Ti alloys; one was fine Ti precipitates which were less than 0.1 μm in size, and the other was large

author's e-mail: miyazawa.takeshi@LHD.nifs.ac.jp

Table 1 Chemical composition for the alloys (mass%).

Code	Scale	Cr	Ti	Y	C	N	O
V-4Cr-4Ti-0.008O	30 g	3.87	4.02	<0.02	0.005	0.006	0.008
V-4Cr-4Ti-0.010O	30 g	4.25	4.48	<0.02	0.007	0.008	0.010
V-4Cr-4Ti-0.019O	166 kg	4.11	4.15	<0.02	0.025	0.009	0.019
V-4Cr-4Ti-0.051O	15 kg	4.40	4.51	-	0.014	0.015	0.051
V-4Cr-4Ti-0.11O	30 g	4.27	4.46	<0.02	0.014	0.015	0.11
V-4Cr-4Ti-0.12O	200 g	4.00	4.11	<0.01	0.012	0.010	0.12
V-4Cr-4Ti-0.18O	30 g	4.24	4.42	<0.02	0.009	0.018	0.18
V-4Cr-4Ti-0.36O	30 g	3.90	3.96	<0.02	0.010	0.016	0.36
V-4Cr-4Ti-0.080N	30 g	3.91	3.89	<0.01	0.016	0.080	0.019
V-4Cr-4Ti-0.26N	30 g	3.85	3.96	<0.02	0.013	0.26	0.020
V-4Cr-4Ti-0.29N	30 g	3.93	4.07	<0.01	0.013	0.29	0.025
V-4Cr-4Ti-Y-0.009O	15 kg	4.23	4.17	0.11	0.011	0.009	0.009
V-4Cr-4Ti-Y-0.027O	30 g	4.01	4.07	0.12	0.007	0.002	0.027
V-4Cr-4Ti-Y-0.070O	30 g	3.28	3.96	0.01	0.014	0.014	0.070
V-4Cr-4Ti-Y-0.11O	30 g	3.86	4.01	0.01	0.017	0.019	0.11
V-4Cr-4Ti-Y-0.17O	30 g	3.54	3.88	0.004	0.014	0.024	0.17
V-4Cr-4Ti-Y-0.21O	30 g	3.89	3.97	0.02	0.013	0.019	0.21
V-4Cr-4Ti-Y-0.03O	30 g	4.23	3.92	0.08	0.021	0.023	0.030
V-4Cr-4Ti-Y-0.27O	15 kg	3.87	3.99	0.06	0.010	0.018	0.27
V-4Cr-4Ti-Y-0.36O	30 g	4.19	3.89	0.02	0.013	0.021	0.36
V-4Cr-4Ti-Y-0.082N	30 g	3.38	4.27	0.20	0.016	0.082	0.015
V-4Cr-4Ti-Y-0.24N	30 g	4.28	4.56	0.19	0.011	0.24	0.017
V-4Cr-4Ti-Y-0.26N	30 g	3.60	4.27	0.20	0.018	0.26	0.022

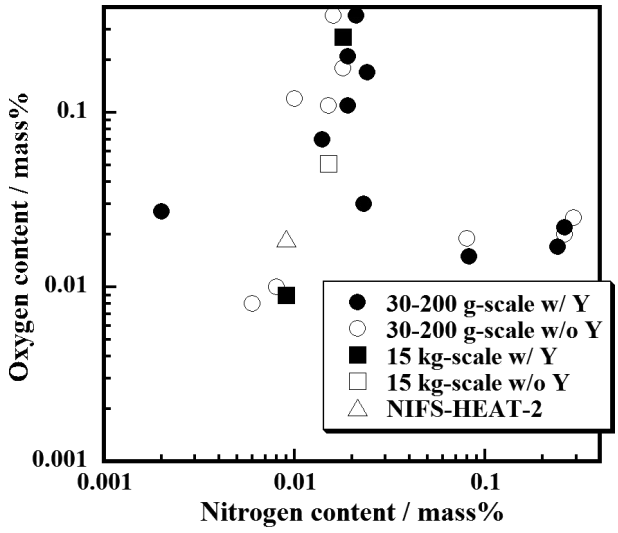

Fig. 1 N and O contents of the alloys used in the present study. Open circles, square and triangle show N and O contents for V-4Cr-4Ti alloys. Closed circles and squares show N and O contents for V-4Cr-4Ti-Y alloys.

Ti precipitates which were not less than 0.1 μm nor more than 0.5 μm in size [10]. Large precipitates were already present after hot rolling, following melting. In the previous study, annealing as-melted NIFS-HEAT-2 at 950°C for 3.6 ks resulted in the formation of these precipitates [11]. Fine precipitates were formed at 700°C and disappeared at 1100°C. It is assumed that TiN and V_2O_5 were decomposed during melting, and then the dissolved N and O were precipitated during fabrication and annealing.

Miniature tensile specimens with a gauge size of $1.2 \times 5 \times 0.25$ mm were used for tensile tests. Miniaturized Charpy specimens were prepared with dimensions of $1.5 \times 1.5 \times 20$ mm, a notch angle of 30°, and a notch depth of 0.3 mm, so that ligament size was 1.2 mm. The specimens were annealed at 1000°C for 7.2 ks for V-4Cr-4Ti alloys, and at 950°C for 3.6 ks for V-4Cr-4Ti-Y alloys in a vacuum better than 1×10^{-4} Pa. The grain size of each specimen after annealing was less than 30 μm. Tensile tests were performed at RT at an initial strain rate of $6.67 \times 10^{-4}\ s^{-1}$. Microstructural observations were carried out using transmission electron microscopy (TEM). Charpy impact tests were conducted from −196°C to RT using an instrumented Charpy impact test machine at International Research Center for Nuclear Materials Science, Tohoku University. The crosshead speed of Charpy impact tests was 5 m/s. Fracture surfaces were analyzed using scanning electron microscopy (SEM).

3. Results

3.1 Tensile properties

Figure 2 plots the dependence of yield stress (YS) and ultimate tensile strength (UTS) on O and N contents at RT. YS and UTS for pure vanadium were also plotted for comparison [2]. Harrod and Gold reported that YS and UTS for pure vanadium linearly increased with increasing O and N contents in this range. The hardening coefficient per unit of O content was 1900 MPa/mass% and that of N content was 2500 MPa/mass%. No precipitates due to O and N doping were observed in the microstructure for pure vanadium; thus, the hardening of pure vanadium was caused by solid

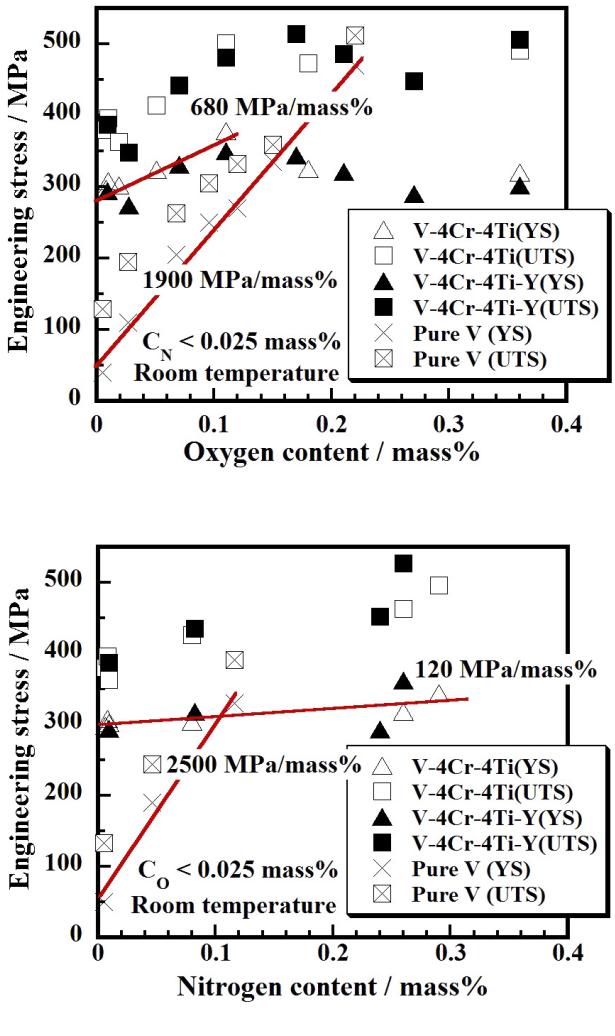

Fig. 2 Dependence of YS and UTS on O and N contents.

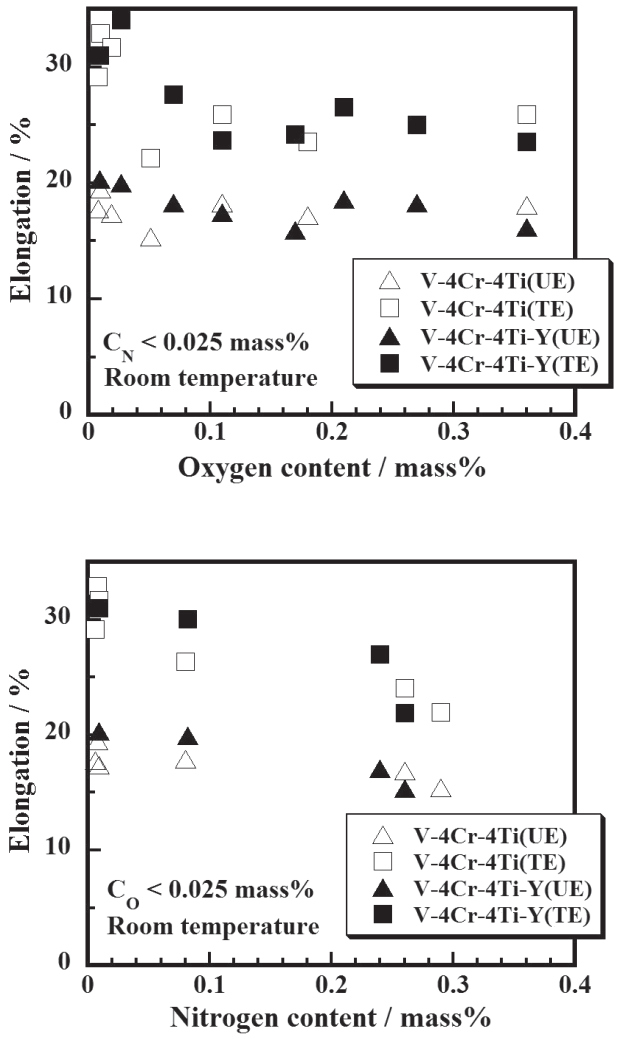

Fig. 3 Dependence of UE and TE on O and N contents.

solution hardening by interstitial O and N. The dependence of YS and UTS for V-4Cr-4Ti alloys on O and N contents was similar to that for V-4Cr-4Ti-Y alloys. Y addition had little effect on YS and UTS of V-4Cr-4Ti alloys at RT. YS and UTS for the vanadium alloys linearly increased with increasing O content up to 0.1 mass%. The hardening coefficient per unit of O content was 680 MPa/mass%, which was much less than that for pure vanadium. YS and UTS for the vanadium alloys did not increase above 0.1 mass% in O content, but increased gradually with increasing N content up to 0.29 mass%. The hardening coefficient per unit of N content was 120 MPa/mass%. The hardening in V-4Cr-4Ti alloys by N was less than that by O.

Figure 3 plots the dependence of uniform elongation (UE) and total elongation (TE) on O and N contents at RT. All the data on UE exceeded 15% in the range of O and N contents in the present study. The previous tensile tests at RT on unalloyed vanadium (pure vanadium) indicated that the threshold content of N for embrittlement (defined as UE = 0%) was 0.24 mass% [5]. Alloying suppressed embrittlement due to N doping.

3.2 TEM observation

Figure 4 presents bright field TEM images for vanadium alloys doped with O. Statistical analysis for the size distribution of precipitates is presented in Fig. 5. It has been reported that two kinds of precipitates (fine and large) were observed in TEM images of the NIFS-HEAT-2 specimens annealed at 1000°C [12]. The size of fine precipitates was less than 0.1 μm and that of large precipitates was not less than 0.1 μm nor more than 0.5 μm. These precipitates were observed in V-4Cr-4Ti-0.11O, V-4Cr-4Ti-0.18O, V-4Cr-4Ti-Y-0.21O, and V-4Cr-4Ti-Y-0.27O alloys. Comparison of the distribution for V-4Cr-4Ti-0.11O and V-4Cr-4Ti-0.18O alloys indicates clear that the number of fine precipitates increased with increasing O content. The number density of precipitates increased with increasing O content in V-4Cr-4Ti alloy. Coarse precipitates with 0.5 μm or larger were observed in V-4Cr-4Ti-Y-0.27O alloy. Such coarse precipitates were not observed in alloy with high O content (V-4Cr-4Ti-Y-0.21O alloy). These precipitates are considered to be Y_2O_3 inclusions [7, 13].

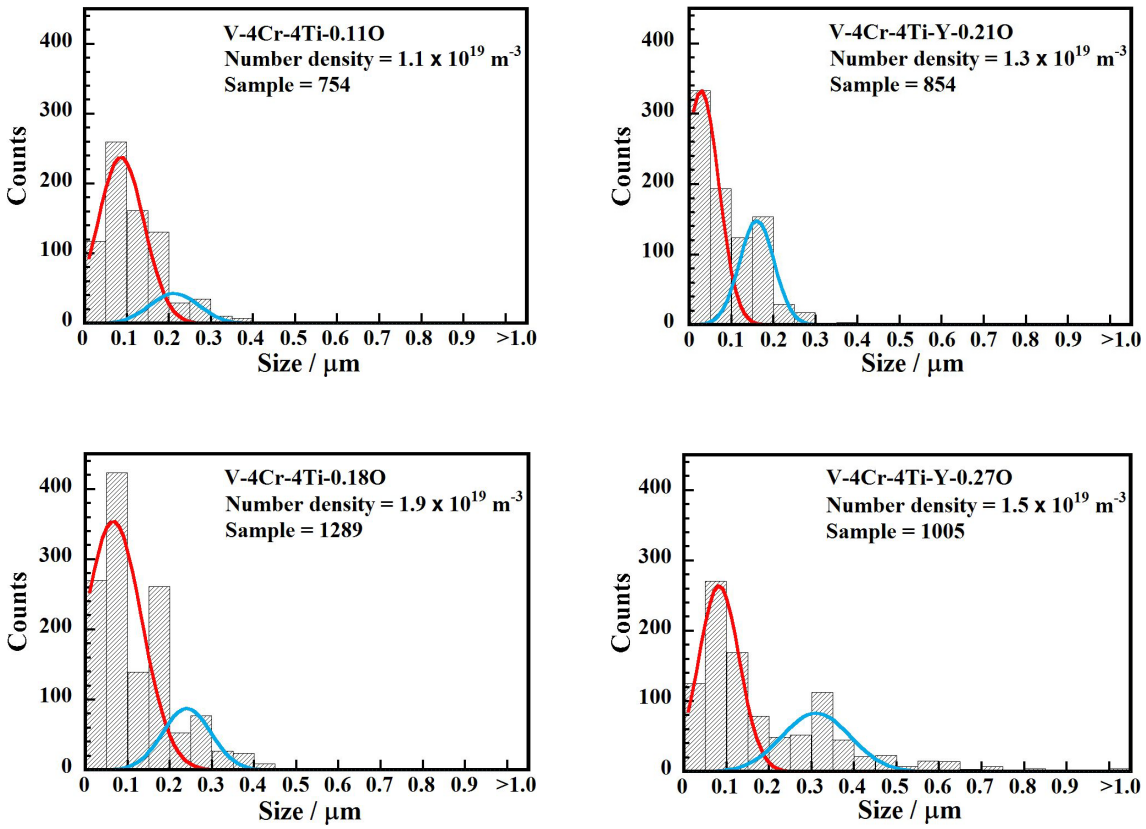

Fig. 5 Size distribution of precipitates for vanadium alloys doped with O. Red and blue solid line exhibit Gaussian profiles for smaller (Peak A) and larger (Peak B) precipitates, respectively.

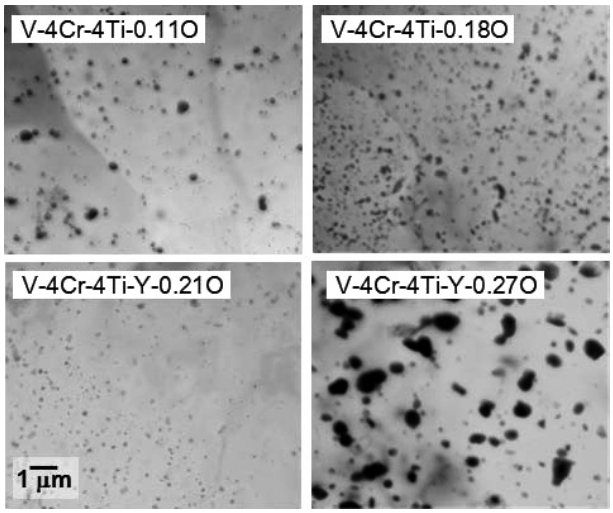

Fig. 4 TEM images for vanadium alloys doped with O.

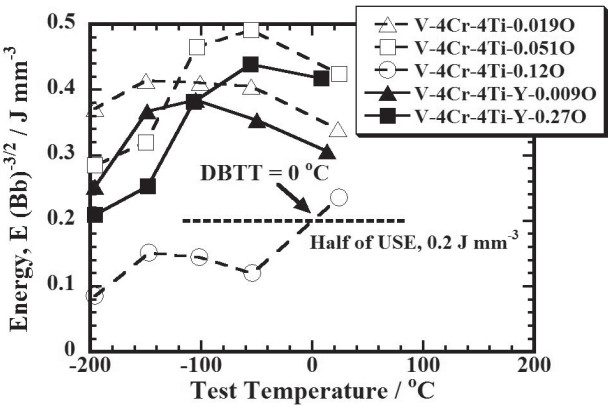

Fig. 6 Absorbed energy in the Charpy impact tests.

3.3 Charpy impact properties

Figure 6 plots absorbed energies from −196°C to RT. These energies are normalized by specimen width (B = 1.5 mm) and ligament size (b = 1.2 mm). In the present study, ductile-to-brittle transition temperature (DBTT) is defined as the temperature where the absorbed energy is half of the upper-shelf energy (USE). Table 2 summarizes USEs and DBTTs for the alloys tested in the present study. DBTTs for the alloys, except for V-4Cr-4Ti-0.12O alloy, were below −196°C. The data for V-4Cr-4Ti-0.12O alloy were insufficient to determine USE for that alloy. Assuming USE is the average value (0.40 J/mm^3) of USEs for the other alloys, DBTT for V-4Cr-4Ti-0.12O alloy was estimated as 0°C. Figure 7 presents SEM images of the fracture surfaces of V-4Cr-4Ti-0.12O and V-4Cr-4Ti-Y-0.27O alloys. At RT and −56°C, the fracture surfaces of V-4Cr-4Ti-Y-0.27O alloy exhibited good ductility with 29% in

Table 2 Summary of Charpy impact properties.

Code	USE (J/mm^3)	DBTT (^{o}C)	Comment
V-4Cr-4Ti-0.019O	0.39	below -196	
V-4Cr-4Ti-0.051O	0.46	below -196	
V-4Cr-4Ti-0.12O	(0.40)*	0	High O doping induced embrittlement.
V-4Cr-4Ti-Y-0.009O	0.35	below -196	
V-4Cr-4Ti-Y-0.27O	0.41	below -196	Y addition suppressed embrittlement due to O doping.

*Assuming that the USE for V-4Cr-4Ti-0.12O is 0.40 J/mm^3 which is the average value of USEs for the other alloys.

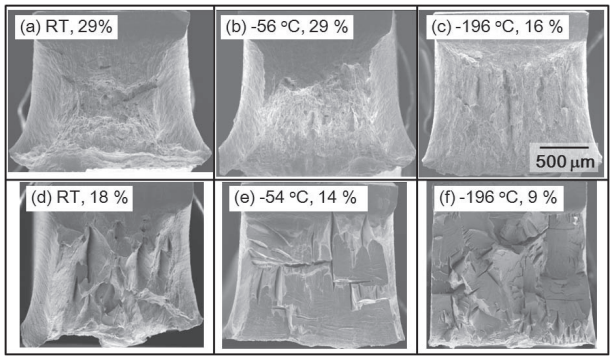

Fig. 7 SEM images for fracture surface (a), (b), (c) for V-4Cr-4Ti-Y-0.27O alloy and (d), (e), (f) for V-4Cr-4Ti-0.12O alloy. Test temperature and data for lateral expansion are indicated.

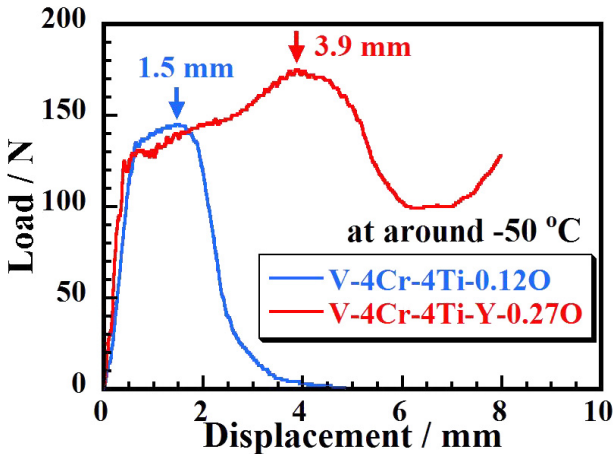

Fig. 8 Load-displacement curves at around −50°C for V-4Cr-4Ti-Y-0.27O and V-4Cr-4Ti-0.12O alloys. Arrows indicate crack initiation points.

lateral expansion ratio (LE). The fracture surface of V-4Cr-4Ti-Y-0.27O alloy at −196°C and that of V-4Cr-4Ti-0.12O alloy at RT were a mixture of ductile fractures with dimples and brittle fractures with secondary cracks. At −54 and −196°C, the fracture surface of V-4Cr-4Ti-0.12O alloy indicated fully brittle fracture characterized by cleavage and secondary crack with random directions. Figure 8 plots load-displacement curves at around −50°C for V-4Cr-4Ti-Y-0.27O and V-4Cr-4Ti-0.12O alloys. No difference in YS at around −50°C was observed for these alloys. The crack initiation point is defined as the displacement at maximum load on the load-displacement curve. The displacements at crack initiation for V-4Cr-4Ti-0.019O, V-4Cr-4Ti-0.051O and V-4Cr-4Ti-Y-0.009O alloys exceeded 4 mm. Crack initiation for V-4Cr-4Ti-Y-0.27O alloy occurred at 3.9 mm in displacement, while that for V-4Cr-4Ti-0.12O alloy occurred at 1.5 mm. In these alloys highly doped with O, displacement for crack initiation was increased by Y addition.

4. Discussion

The linear increase in YS is caused by solid solution hardening due to N and O doping. The hardening coefficient for vanadium alloys was smaller than that for pure V because of the formation of Ti-CON precipitates according to the previous study [12]. In a previous study for the effect of impurities after liquid lithium exposure [14], precipitates were effectively formed even though significant N contamination occurred. It is, therefore, assumed that the hardening coefficient of N doping (120 MPa/mass%) was smaller than that of O doping (680 MPa/mass%). The amount of O in precipitates can be estimated from the total volume of the precipitates. Assuming the precipitates are spherical, the total volume V of precipitates is given as

$$V = N_A \times \left(\frac{4\pi}{3}\right)\left(\frac{\mu_A}{2}\right)^3 + N_B \times \left(\frac{4\pi}{3}\right)\left(\frac{\mu_B}{2}\right)^3, \quad (1)$$

$$N = N_A + N_B, \quad (2)$$

where N_A is the number density of smaller (Peak A) precipitates, N_B is the number density of larger (Peak B) precipitates, μ_A is the mean size of the precipitates with Peak A, μ_B is the mean size of the precipitates with Peak B. Table 3 lists estimated O content in precipitates determined using a mass density for TiO (4.93 g/cm^3) and TiO_2 (4.26 g/cm^3) [15]. Assuming the precipitates are TiO_2, all the O in the alloys doped with O is scavenged as TiO_2 precipitates from the alloy matrix. It is thus assumed that precipitation is enhanced, and then solid solution hardening is saturated above 0.1 mass% in O content. Because Ti precipitates are formed depending on O content regardless of

Table 3 Estimated oxygen content in precipitates.

Code	Volume fraction of precipitates (Vol. %)	Oxygen content in precipitates (mass%)
V-4Cr-4Ti-0.11O	1.2	0.24 (TiO) 0.34 (TiO_2)
V-4Cr-4Ti-0.18O	2.8	0.56 (TiO) 0.77 (TiO_2)
V-4Cr-4Ti-Y-0.21O	1.0	0.19 (TiO) 0.26 (TiO_2)
V-4Cr-4Ti-Y-0.27O	8.5	1.3 (TiO) 2.4 (TiO_2)

Y, Y addition had little effect on YS and UTS of V-4Cr-4Ti alloys. Precipitates in V-4Cr-4Ti alloys were, however, identified as TiO in previous study [12]. Further study is necessary to determine whether TiO_2 precipitates formed.

Coarse precipitates were observed in V-4Cr-4Ti-Y-0.27O alloy, but not in alloy with high O content (V-4Cr-4Ti-Y-0.21O alloy), as shown in Fig. 4. In V-4Cr-4Ti-Y-0.21O alloy, Y had little effect on precipitation, probably because of low residual Y (0.02 mass%). The reasons for the low residual Y are thought to be as follows: (1) Slag-out could effectively work in V-4Cr-4Ti-Y-0.21O alloy because the distance from the center of the melt to the surface is less than that of V-4Cr-4Ti-Y-0.27O alloy due to the difference in melting scale. (2) The difference in stirring conditions due to the melting scale changed the efficiency of slag-out. A large amount of Y, therefore, remained in the larger scale ingot (V-4Cr-4Ti-Y-0.27O alloy). Y_2O_3 inclusions remained in the melted V-4Cr-4Ti-Y-0.27O alloy.

In Charpy impact test, Y addition improved absorbed energy in alloys highly doped with O, but did not affect YS below RT. Y addition did not suppress hardening due to O doping, but increased the displacement where crack initiation occurred. These results indicate that Y addition increased the deformation for crack initiation. The absorbed energies for V-4Cr-4Ti-0.12O alloy decreased because precipitates likely induced crack initiation. It is assumed that precipitates for V-4Cr-4Ti-0.12O alloy could be coarsened or be formed with higher number density, compared with V-4Cr-4Ti-Y-0.27O alloy with 0.06 mass% Y, where the precipitates did not degrade the impact energy. Y addition exceeding 0.3 mass%, however, formed many coarse inclusions, which also degraded the impact energy [16]. It is assumed that residual Y (0.05–0.1 mass%) is appropriate for maintaining favorable impact properties.

5. Summary

The effects of Y addition on mechanical properties of V-4Cr-4Ti alloys with high O and N contents were investigated. Ti precipitates increased with increasing O, regardless of Y. Y addition had little effect on YS and UTS of V-4Cr-4Ti alloys at RT but improved impact properties in alloys highly doped with O. Y addition did not suppress hardening due to O doping but did increase deformation for crack initiation.

Acknowledgments

The authors are grateful to Mr. T. Onda of the Onda Kougyo Co., Ltd., for support in fabricating button alloys. This work is supported by Research Fellowships of the Japan Society for the Promotion of Science for Young Scientists.

[1] T. Muroga, Comprehensive Nuclear Materials **4**, 391 (2012).
[2] D.L. Harrod *et al.*, International Metals Reviews **25**, 163 (1980).
[3] J.F. Smith, *Phase Diagrams of Binary Vanadium Alloys* (ASM International, 1989).
[4] D.L. Smith *et al.*, J. Nucl. Mater. **135**, 125 (1985).
[5] T. Kainuma *et al.*, J. Nucl. Mater. **80**, 339 (1979).
[6] M.L. Grossbeck *et al.*, J. Nucl. Mater. **258**, 1369 (1998).
[7] T. Nagasaka *et al.*, J. Nucl. Mater. **367**, 823 (2007).
[8] T. Nagasaka *et al.*, Fusion Technol. **39**, 659 (2001).
[9] T. Nagasaka *et al.*, J. Plasma Fusion Res. SERIES **5**, 545 (2002).
[10] N.J. Heo *et al.*, J. Nucl. Mater. **307**, 620 (2002).
[11] T. Nagasaka *et al.*, Fusion Eng. Des. **61**, 757 (2002).
[12] N.J. Heo *et al.*, J. Nucl. Mater. **325**, 53 (2004).
[13] T. Miyazawa *et al.*, J. Nucl. Mater. **442**, S341 (2013).
[14] T. Nagasaka *et al.*, Fusion Eng. Des. **81**, 307 (2006).
[15] Chemical Handbook (the Chemical Society of Japan, 2004) [in Japanese].
[16] T. Chuto *et al.*, J. Nucl. Mater. **326**, 1 (2004).